MULTI-ANGLE HYPERSPECTRAL OBSERVATIONS USING FLUORESENCE AND *PRI* TO DETECT PLANT STRESS AND PRODUCTIVITY IN A CORNFIELD

Elizabeth M. Middleton[1], Yen-Ben Cheng[2], Petya E. Campbell[3], K. Fred Huemmrich[3], Lawrence A. Corp[4], Sergio Bernardes[5], Qingyuan Zhang[6], David R. Landis[7], William P. Kustas[8], Craig S. T. Daughtry[8], Joseph G. Alfieri[8], and Andrew L. Russ[8]

1. Biospheric Sciences Laboratory, NASA/Goddard Space Flight Center, Greenbelt, MD 20771, USA; Elizabeth.M.Middleton(at)nasa.gov
2. Formerly; Sigma Space Inc., Lanham, MD 20706, USA; currently: Ceres Imaging, 2146 3rd Street, San Francisco, CA 94107, USA; Yen-Ben.Cheng(at)gmail.com
3. Joint Center for Earth Tech., University of Maryland at Baltimore County, Baltimore, MD 21228, USA; {Petya.K.Campbell / Karl.F.Huemmrich}(at)nasa.gov
4. System Science and Applications, Inc., Lanham, MD 20706, USA; Lawrence.A.Corp(at)nasa.gov
5. NPP Fellow, NASA/Goddard Space Flight Center, Greenbelt, MD 20771, USA; Sergio.Bernardes(at)nasa.gov
6. Universities Space Research Association, Columbia, MD 21045, USA; Qingyuan.Zhang-1(at)nasa.gov
7. Global Science & Technology, Inc., Greenbelt, MD 20770, USA; David.R.Landis(at)nasa.gov
8. USDA-ARS Hydrology and Remote Sensing Laboratory, Beltsville Agricultural Research Center, Beltsville, MD 20705, USA; {Bill.Kustas / Craig.Daughtry / Joe.Alfieri / Andrew.Russ }(at)ars.usda.gov

ABSTRACT

The effects of seasonal water stress and nitrogen availability, which significantly impact plant productivity, can be monitored remotely using reflectance and fluorescence measurements which are commonly acquired under varying viewing and illumination geometries. During the growing seasons of 2012 and 2014, we collected canopy fluorescence, hyperspectral reflectance spectra, and biophysical measurements in corn plots established for nitrogen (N) and water augmentation within a USDA/Beltsville experimental cornfield also hosting an eddy covariance flux tower. There were four N application levels (0% N, 50% N, 100% N, 200% N) of the optimal level of 140 kg/ha, and two water availabilities (watered, not-watered) to produce eight treatment plots.

We examined the behaviour of the Solar Induced Fluorescence (*SIF*) and the Photochemical Reflectance Index (*PRI*) during morning and afternoon periods for nine days throughout the 2012 growing season, including early, vegetative, reproductive, and senescent phenological growth stages. The *SIF* was retrieved from high resolution spectra using the 3-wavelength Fraunhofer Line Depth method in both oxygen absorption bands associated with the two chlorophyll fluorescence peaks in the red at 687 nm and the far-red at 760 nm. *PRI* was calculated as a Normalized Difference Reflectance Index using two wavelengths at 531 and 570 nm.

At each collection, directional measurements were obtained for the *SIF*s and *PRI* at 15° view-zenith angle increments along the solar principal plane, in order to quantify the maximum anisotropy associated with the cornfield's bidirectional reflectance and fluorescence distribution functions. Along the solar principal plane, the maximum and minimum values at the hotspot and the coldspot, respectively, were determined and used to calculate an Anisotropy Difference Index (*ANDI*) as coldspot minus hotspot. We found that the various *SIF* values and *PRI* all exhibited significant anisotropy across the growing season, and these seasonal *ANDI* profiles differed significantly among these four observation types. Anisotropy for far-red SIF_{760} always exceeded that for

DOI: 10.12760/02-2015-2-03

red SIF_{687} (<0.001 W/(m^{2}sr)), at each phenologic stage, and was greatest in mid-season during early reproductive phases. Also at mid-season, *ANDI* was highest for the *SIF* Ratio (SIF_{687}/SIF_{760}) but lowest for the *PRI*. *ANDI* for *SIF*s was most variable for watered plots over the season. Nitrogen application rates did not significantly affect the observed anisotropy. We include examples of data acquired in 2014 for cornfield anisotropy obtained with our custom tower-mounted FUSION system, and the new FluoWat leaf clip.

Keywords: Hyperspectral, fluorescence, anisotropy, *PRI*, *SIF*, corn.

INTRODUCTION

The magnitude of the spectral radiance scattered from a vegetated canopy is known to be affected by the viewing and illumination geometries (e.g., (1,2)), causing canopy exitance to differ from a uniform isotropic state. Anisotropy occurs when directional radiances are unequal, which is usually most pronounced in the solar principal plane (*SPP*). This anisotropy for the reflected radiation from the hemisphere associated with the vegetation is expressed as the Bidirectional Reflectance Distribution Function (*BRDF*). The normalized *BRDF* expressing anisotropy in the *SPP* typically exhibits a maximum value in the backscatter direction (e.g., -10° to -60°) at the anti-solar point referred to as the hotspot (*HS*). This typically occurs where the backscatter view zenith angle (*VZA*) and the solar zenith angle (*SZA*) are equal (*VZA* ≈ *SZA*). A minimum value occurs in the forward scattered direction (e.g., +10° to +60°), at a variable position influenced by canopy composition and density, as well as view/illumination geometry. To avoid these complications, the nadir (or middle) value in the *SPP* (where *VZA* = 0) is typically preferred in remote sensing studies to minimize variations among observations acquired at different times and locations, and to minimize atmospheric effects by having the shortest path length between surface and remote sensor.

Nevertheless, non-nadir observations are often acquired by instruments on satellites (e.g., MODIS on Terra and Aqua), so that a *BRDF* normalization to estimate nadir values is commonly employed. These *BDRF*s are well-established for reflected radiation at coarse spatial scales, for many surface types. For example, the MODIS algorithm to estimate nadir reflectance from directional observations uses the Ross-Thick/Li-Sparse semi-empirical model (3). However, the Bidirectional Fluorescence Distribution Function (*BFDF*) properties of canopy fluorescence emissions are poorly understood and characterized. Since remote sensing observations of Solar Induced Fluorescence (*SIF*) have now been achieved from satellites, especially those with large footprints and variable viewing directions (e.g., GOSAT and Metop (4)), and at different times of the day (i.e., different illumination and environmental conditions), there is a need to determine the relative expression of isotropy vs. anisotropy of *SIF*, for a variety of vegetation types and conditions. Here, we incorporate anisotropy analysis for *SIF* into our field studies at a USDA research cornfield, building on two decades of measurements, which has had a special focus on the *PRI* and *SIF* (5,6,7,8,9,10,11,12,13,14,15,16,17,18,19,20,21,22,23,24,25,26,27,28,29,30).

Results from the 2012 and 2014 field seasons are presented here.

METHODS

The research cornfield is located in Beltsville, MD, USA and managed by the United States Department of Agriculture–Agricultural Research Service (USDA-ARS). The field was planted with corn (*Zea mays* L.; variety, Pioneer 33A14) in late May 2012. For this study, we utilized the permanent nitrogen (N) plots that were established over a decade ago which are provided one of four N application levels (0%N, 50%N, 100%N, and 200%N of the optimal 140 kg/ha).

In 2012, the USDA-ARS doubled the experimental plot variation by adding water treatments (watered and not-watered). Each N plot was divided in half, into ~15 m × 15 m sub-plots. An irrigation system was installed to supply parallel drip lines that were laid at 0.3 m intervals throughout those half plots designated for water augmentation. Thus, eight treatment plot types were established,

with replicates, where each of the N plots (0% N, 50% N, 100% N and 200% N) had a rain-fed only half plot (not-watered) and a water-augmentation (watered) half plot. Note, all of the plots (watered and not-watered) received rainfall. In addition to these experimental treatments, the study site experienced unseasonably high and sustained daytime temperatures (>32°C) with little precipitation (i.e., severe drought conditions) for the first half of the growing season. We examined the red and far-red *SIF* and the Photochemical Reflectance Index (*PRI*) for stress responses as part of a longer-term experiment at this cornfield.

For the eight treatment plots, we examined the *SPP* anisotropy of the *PRI*, a reflectance index which exhibits significant anisotropy under environmental stress conditions (31), along with the *SPP* anisotropy for both *SIF* bands, red SIF_{687} and far-red SIF_{760}. The canopy *SIF* retrievals were obtained with a pole-mounted high-resolution spectrometer (Ocean Optics HR 4000, Dunedin, FL, USA) at mid-mornings and mid-afternoons. The canopy spectra used for *PRI* calculations were made contemporaneously with an ASD FieldSpec spectroradiometer (ASD Inc. Boulder, CO, USA). These canopy spectra were acquired at seven *VZA*s along the *SPP*: nadir (0°), ±15°, ±30°, ±45°, and ±60°. Reference spectra were collected over a Spectralon panel (Labsphere, Inc. North Sutton, NH, USA). These canopy and reference spectra were used to compute:

(i) *PRI*, as a normalized difference reflectance index using two green bands centred at 531 and 570 nm ($PRI = (R531 - R570)/(R531 + R570)$; and

(ii) *SIF* retrievals performed in the O_2-B and O_2-A atmospheric oxygen absorption bands centred at 687 and 760 nm, respectively, using the 3*FLD* (3-wavelength Fraunhofer Line Depth) retrieval approach (32) to obtain SIF_{687} and SIF_{760}, and their ratio (SIF_{687}/SIF_{760}).

An example of the spectra used for *SIF* retrievals is given in Figure 1.

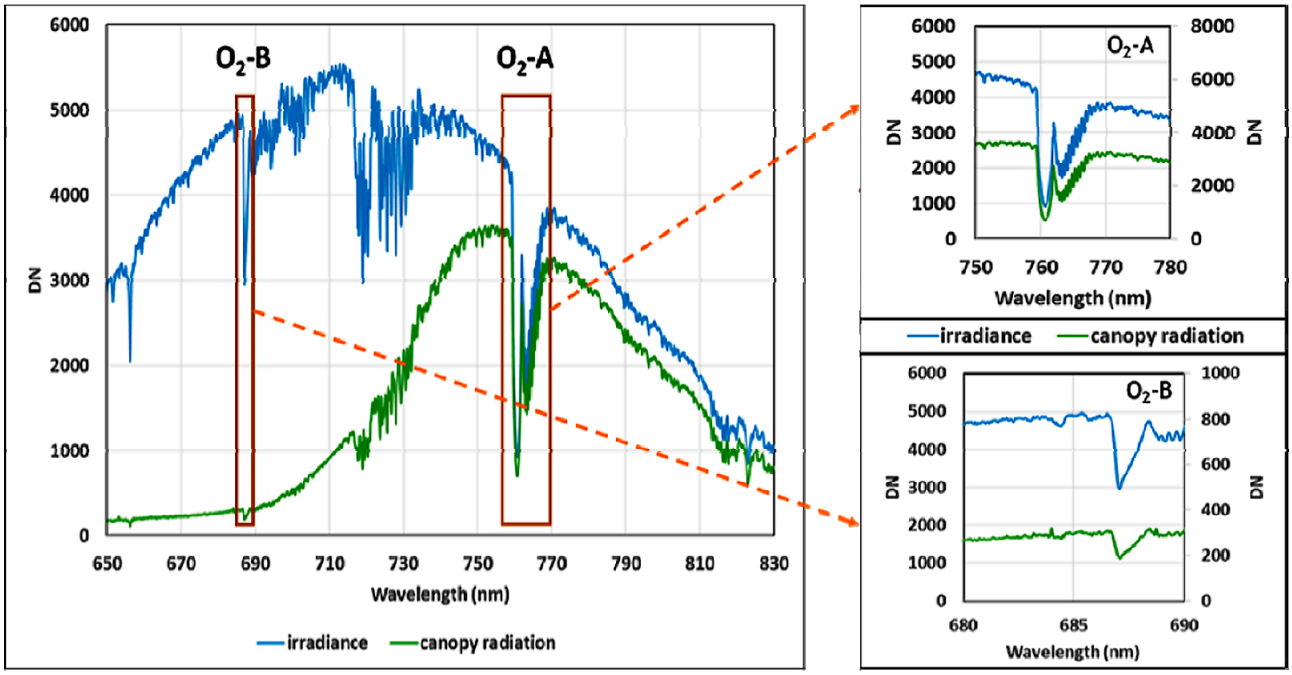

Figure 1: Examples of spectra (in digital numbers, DN) obtained in the cornfield and used for retrieval of solar induced chlorophyll fluorescence (SIF). The left panel gives the upwelling radiance measured 1 m above the corn canopy (green), and the downwelling irradiance (blue) obtained from the horizontally placed Spectralon reference panel, both obtained using nadir views. The right panels provide the spectral regions used for SIF retrievals in the O_2-A band (top panel) and the O_2-B band (bottom panel) where the DNs for the irradiance spectrum (blue) are given to the left and those for the vegetation (green) are on the right.

We produced *BRDF* and *BFDF SPP* curves in the mornings and the afternoons for the *PRI* and *SIF*-related indices across the growing season for the experimental N/water treatments, obtained from pole-mounted instruments. Directional SIF_{687}, SIF_{760}, and *PRI* observations were acquired in the eight plots during 12 days over the growing season, from which half-day (morning *vs*. afternoon) and daily averages were determined. The *SIF* Ratio (SIF_{687}/SIF_{760}) was also computed for each half day and for daily averages. An anisotropy difference index (*ANDI*) was calculated along the *SPP* from the maximum and minimum values at the hotspot (*HS*) and the coldspot (*CS*), respectively, as their difference (*CS* minus *HS*). *ANDI* values were determined for morning and afternoons, as well as daily averages, for the *SIF* variables and the *PRI*.

USDA-ARS scientists measured carbon, water and energy fluxes using the eddy-covariance method along with meteorological measurements from a tower located in a large rain-fed area of the cornfield with 100% N application. Environmental data such as air temperature and incoming Photosynthetically Active Radiation (*PAR*) were obtained by instruments on the flux tower, in addition to daily Gross Ecosystem Production (*GEP*) determined from half-hourly measurements of CO_2 uptake made with standard eddy covariance techniques (33). In the same field there was a second portable tower on which our custom FUSION system (10,11) was deployed. FUSION has upward and downward viewing spectrometers (Ocean Optics, Dunedin, FL USA) to collect automated hyperspectral radiances to obtain reflectance and *SIF*.

We produced bidirectional *SPP* curves from data acquired in our 2014 campaign with our FUSION system. Examples of morning *BFDF*s acquired in the *SPP*, constructed from directional spectral observations obtained with FUSION spectrometers are shown in Figure 2. Additionally in the summer of 2014, we obtained *in situ* leaf-level measurements of spectral fluorescence for both the leaf tops and bottoms of top-of-canopy (*TOC*) corn leaves using ambient solar radiation in the USDA N/water plots and the custom FluoWat leaf clip (Univ. Valencia, Valencia, Spain) (34) coupled with a FieldSpec spectrometer to obtain chlorophyll fluorescence spectra.

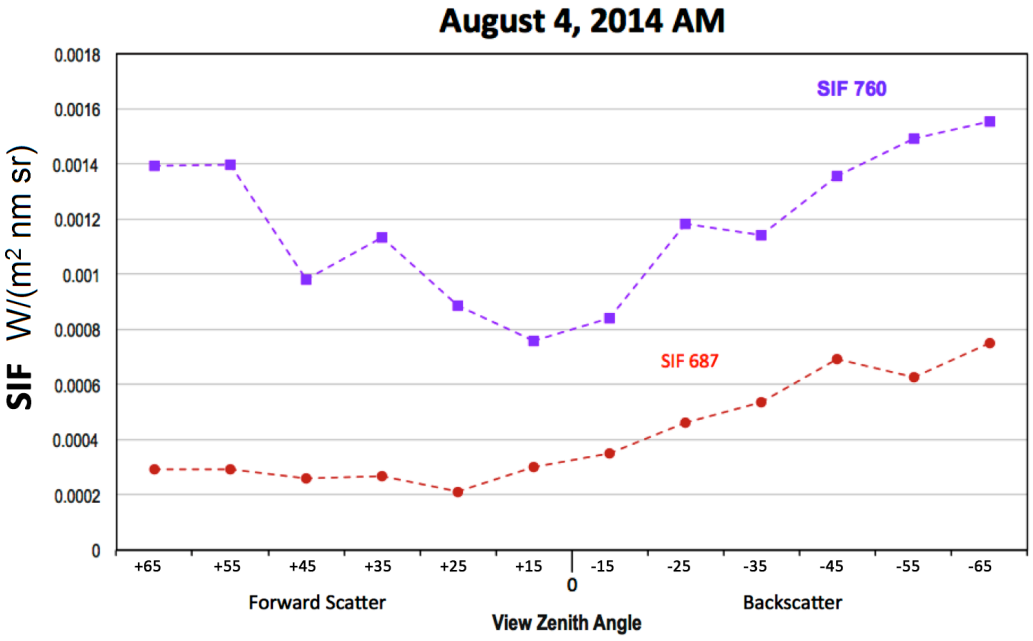

Figure 2: Typical directional response curves in the Solar Principal Plane (SPP) for a ±65° view zenith angle (VZA) range acquired at the USDA cornfield are shown. These observations were acquired in mid-morning on Aug. 4, 2014 with a solar zenith angle of approximately 40°, with our tower-mounted FUSION system, located near the flux tower in a section of the rain-fed (not-watered) cornfield provided with optimal 100% N. These curves show a different magnitude and expression of anisotropy in the SPP: the upper curve, far-red SIF_{760}; lower curve, red SIF_{687}. The backscatter SIF is higher than forward scatter at both wavelengths. The forward scatter for SIF_{687} is low due to re-absorption within the canopy.

RESULTS

The daily *SIF* averages (SIF_{687} and SIF_{760}) for the combined N/water plots were examined across the nine dates in 2012. These SIF observations were normalized with incoming *PAR* to obtain fluorescence yields, also referred to as fluorescence efficiencies (%, Figure 3A). Over the season, the daily SIF_{687} yields varied between ~4 and 6.5% while the SIF_{760} yields varied between ~6 and 9% and had the highest values during the last third of the season associated with early through moderately advanced senescence.

The average SIF_{760} yield exceeded that for the SIF_{687} yield on all dates by 1-4%. Even greater differences between red vs. far-red *SIF* were seen for the daily anisotropy values, *ANDI*, defined as the difference between the cold spot and hot spot values. Averaged over all plots, the daily *ANDI* for SIF_{687} ranged between 0.0006 and 0.0018 W/(m^2 nm sr). Anisotropy was more pronounced (up to 50% higher) with SIF_{760}, for which *ANDI* ranged between 0.0009 and 0.0026 W/(m^2 nm sr) seasonally (Figure 3B).

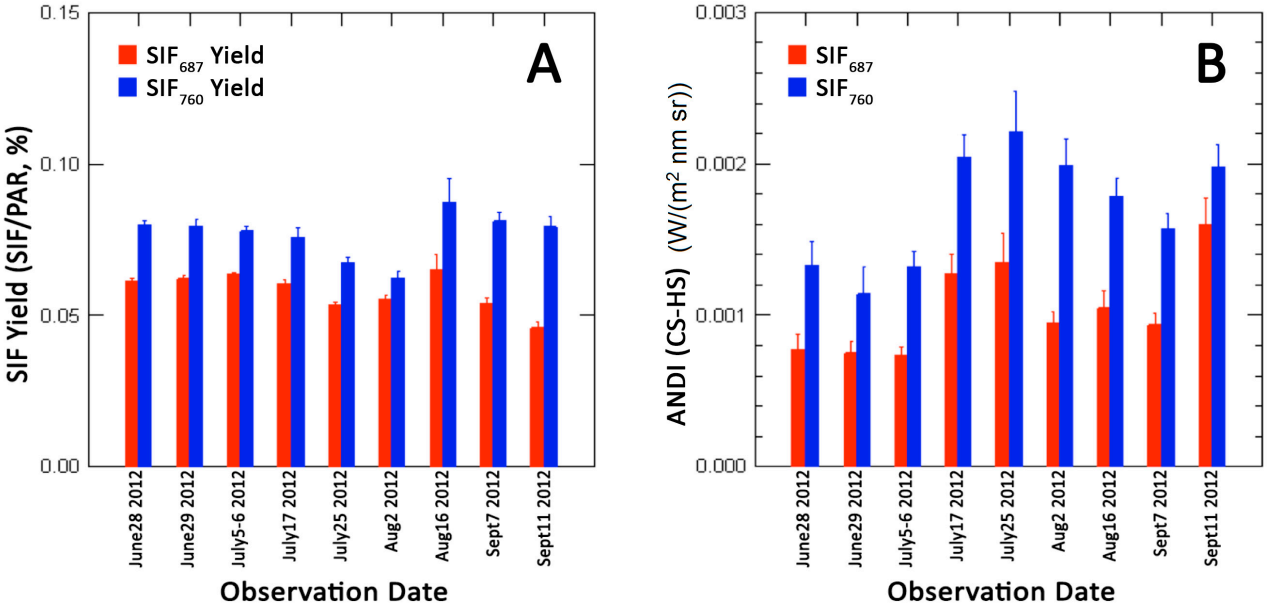

Figure 3: SIF measurements were made at the USDA cornfield on multiple dates throughout the 2012 growing season from late June through mid-September: A) The percent (%) SIF yield was determined for SIF_{687} and SIF_{760}, as the average over all measurements made on each date (all N/water treatments, all directional observations), normalized by the incident daily PAR; B) The anisotropy difference index (ANDI) calculated as the difference between the cold spot and hot spot directional values (CS – HS, W/(m^2 nm sr)). SIF_{760} > SIF_{687} and ANDI for SIF_{760} > SIF_{687} on all dates.

Anisotropy was compared for mornings vs. afternoons and water *vs*. not-watered plots, and grouped into four phenological growth stages: early, vegetative, reproductive, and senescent (Figures 4A, B, C and 5A). Nitrogen plot *ANDI* differences were small so they were not examined further. The *ANDI* values for the *PRI* (Figure 4A) generally declined from the highest early season values through the reproductive stage, and increased again during senescence. The anisotropy for the *PRI* in non-watered plots declined the most, whereas the watered plots were more similar across the season. *ANDI* for SIF_{760} (Figure 4B) displayed a seasonal profile as the plants developed from early to reproductive growth, with a peak *ANDI* observed in the mature reproductive plots. The greatest anisotropy change seasonally for SIF_{760} occurred during mornings in the watered plots, with *ANDI* increasing by a factor of 3 from 0.0008 to 0.0024 W/(m^2 nm sr) (Figure 4B). Lower overall anisotropy was seen for SIF_{687} (average *ANDI*, ~0.001 W/(m^2 nm sr) but which steadily increased over the season (Figure 4B). Consequently, the *ANDI* for the *SIF* Ratio (SIF_{687}/SIF_{760}) exhibited a seasonal peak during the reproductive growth stage for all groups (wa-

tered/not-watered; mornings/afternoons), with higher *ANDI* found in morning observations (Figure 5A). The average seasonal *SIF* Ratio mirrored the seasonal daily *GPP* derived at the eddy covariance tower (Figure 5B).

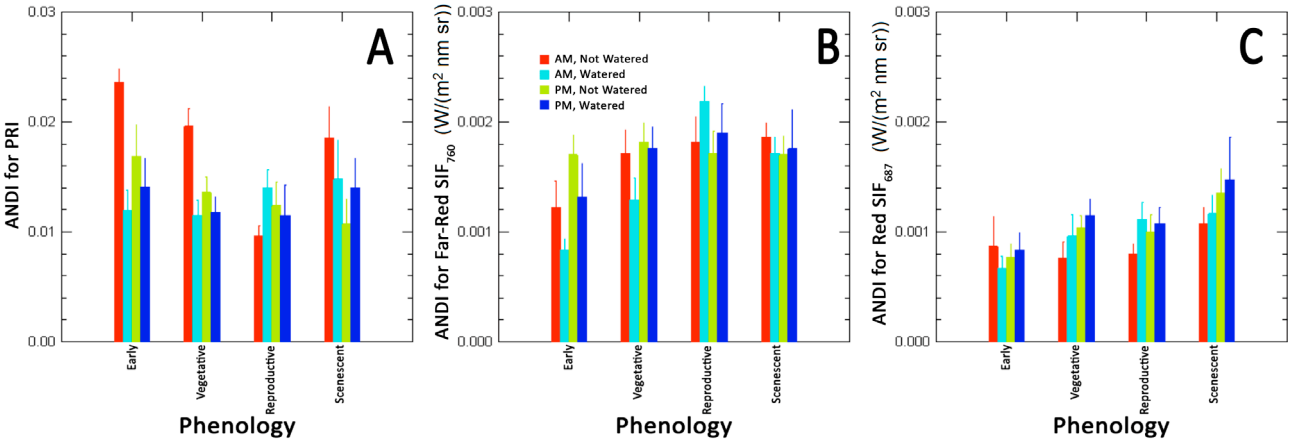

Figure 4: Anisotropy represented by ANDI in the solar principal plane (SPP) varied for the four major phenological growth stages during 2012 at the USDA cornfield: A) PRI; B) SIF_{760}; C) SIF_{687}. The coloured bars show the morning and afternoon averages for the directional observations made in the SPP for the watered (aqua and navy bars) and not-watered (red and lime bars) treatments. No significant differences were observed that could be attributed to the nitrogen treatments. For the PRI, the highest ANDI occurred in the not-watered treatments during mornings, whereas watered plots had generally lower ANDI values, and the seasonal change over all conditions was Δ = 0.009 … 0.0238 units. ANDI for SIF_{760} > SIF_{687}, and SIF_{760} increased by a factor of 3 over the phenological stages (Δ = 0.0012 vs. 0.0018 W/(m² nm sr).

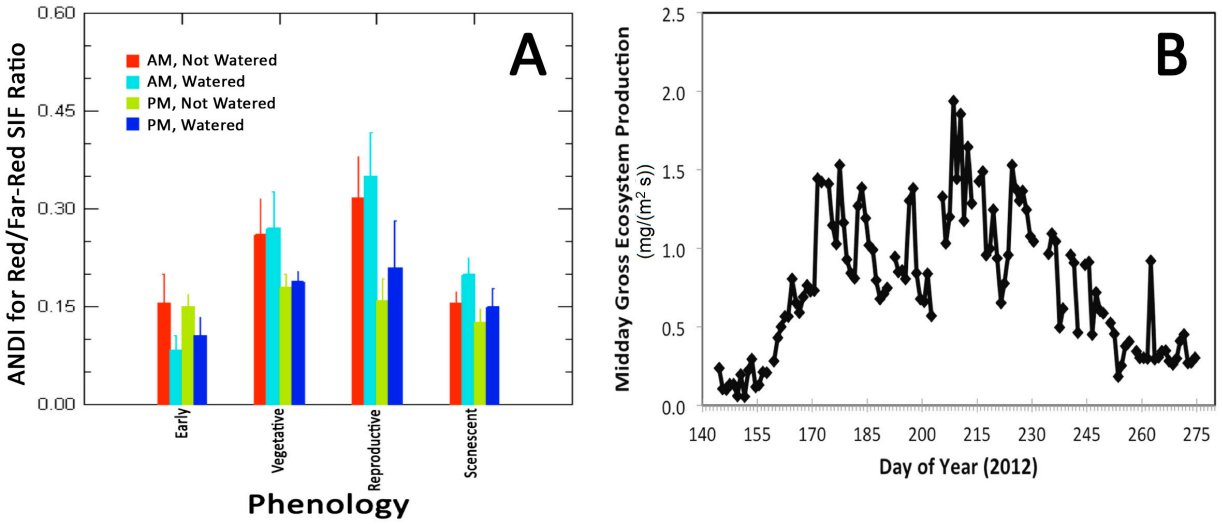

Figure 5: The seasonal trend for the SIF Ratio (SIF_{687}/SIF_{760}) followed the 2012 GEP seasonal profile: A) SIF ratio, Δ = 0.08 … 0.32 units over the season, and the highest ANDI values typically occurred during mornings; B) Midday GEP from eddy covariance across the 2012 season for the 100% N field.

When the *PRI* and SIF_{760} observations obtained from FUSION were combined with the incoming *PAR* and *NDVI* (Normalized Difference Vegetation Index) for the rain-fed (not-watered) 100% N cornfield, a strong correlation (r = 0.89, n = 632) with the flux tower-derived *GEP* was achieved (Figure 6). These spectral data were obtained from FUSION at a fixed VZA (25°), from mid- to late season in 2014 near the eddy covariance tower. Both the FUSION spectral measurements and the tower fluxes were determined at half hourly intervals. In 2014, the corn planting date was delayed until June due to rainy weather conditions.

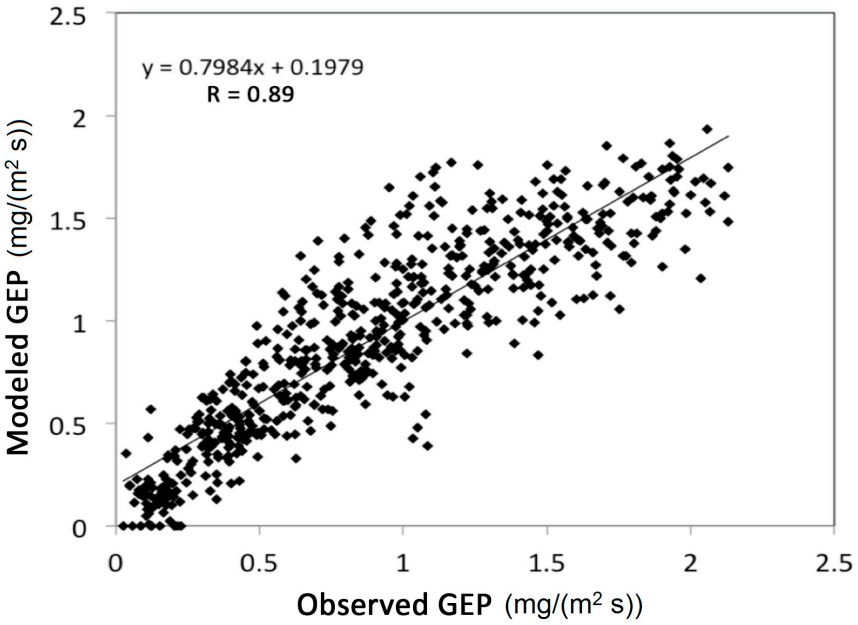

Figure 6: Observed GEP was measured at the eddy covariance tower. The model calculation of GEP used a combination of NDVI, PRI, SIF_{760} and Incident PAR, using observations made at a single view angle (VZA = 25°, N = 632) from the automated FUSION field system at half hourly intervals throughout the latter part of the season (Aug 1 – Oct 15, 2014). The linear correlation between observed and modelled GEP: r = 0.89.

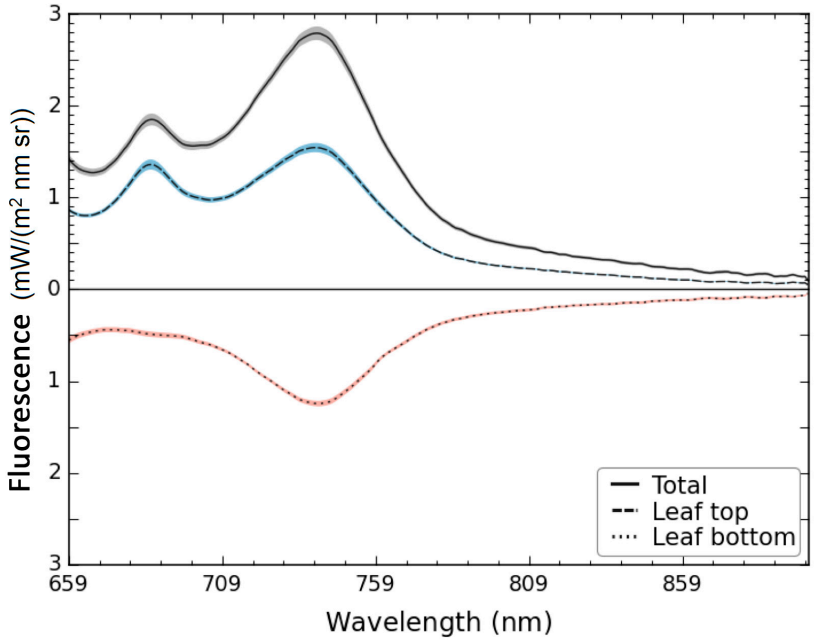

Figure 7: Typical leaf-level fluorescence emission spectra obtained from TOC corn leaves in the USDA plots in 2014. The average upward emission spectrum (from the leaves' upper surfaces) is shown with the blue dashed curve. The downward transmitted emission spectrum measured at the leaves' lower surfaces is shown with the red dotted curve. The total (upward + downward) emission spectrum is shown with the solid black curve. The shaded areas around the mean spectrum indicate the standard error for 5 leaves. The far-red fluorescence (~710 - 770 nm) scattered downward makes a substantial contribution to the with-in canopy radiation.

Fluorescence spectra obtained using the FluoWat leaf clip for *TOC* leaves in the N/water plots revealed that the far-red fluorescence was scattered downward into the canopy at a much greater

rate than the red fluorescence. An example of these corn leaf fluorescence emission spectra is provided in Figure 7. The upward scattered fluorescence was similar for the two peaks at ~1.4 to 1.5 mW/(m^2 nm sr) (**blue curve**). These peak values are ~50% higher than that observed at 760 nm (used for SIF_{760} at canopy scale). However, the downward emissions (**red curve**) showed a different pattern: there was no downward red peak and the downward far-red 740 nm peak (at ~1.3 mW/(m^2 nm sr)) was almost comparable to the upward far-red emission peak, making the upward and downward far-red emissions at wavelengths >710 nm relatively symmetrical relative to the baseline. In contrast, the downward red fluorescence was smooth and much lower in magnitude at ~0.5 mW/(m^2 nm sr). The combined upward and downward emissions (**black curve**) exhibited a substantially higher far-red than red fluorescence: red 685 nm peak, 1.9 mW/(m^2 nm sr): far-red 740 nm peak, 2.8 mW/(m^2 nm sr); and 760 nm, ~2.0 mW/(m^2 nm sr).

DISCUSSION

Understanding the correct interpretation of fluorescence to estimate photosynthetic properties of vegetation has been identified as a critical need for remote sensing (e.g., 35,36). In this field study, we quantified the magnitude of the canopy *SIF* in both the red and far-red *SIF* bands, showing that the diurnal $SIF_{760} > SIF_{687}$ for all dates in this crop. In addition, we demonstrated that the *SPP* anisotropy represented by *ANDI* in these corn canopies was almost 50% higher for SIF_{760} than for SIF_{687}. *ANDI* at both *SIF* wavelengths increased throughout the growth stages, but was not consistently related to either N or water treatments, or to time of day. This may be affected by the commonly observed phenomenon of leaf roll that alters canopy geometry under drought conditions for corn and other crops. When corn leaves roll, the leaf undersides become the surfaces that first intercept incoming light, altering the scattering regime in ways suggested by our FluoWat leaf-level measurements for fluorescence upwelling spectra (where red and far-red peaks are approximately equal) and downwelling spectra (where the red peak << far-red peak) (Figure 7). Our interpretation is that the transmitted red fluorescence is reabsorbed within the canopy and inefficiently utilized in Photosystem I photosynthetic processes, so that a large fraction is re-emitted as excess far-red fluorescence. This is a topic that deserves more attention in future field campaigns.

We have previously shown that the Red/Far-Red *SIF* Ratio (SIF_{687}/SIF_{760}) determined at the nadir *VZA* is linearly related to the canopy's photosynthetic light use efficiency (*LUE*), expressed as the *GEP* normalized to the absorbed *PAR* (*GEP*/*APAR*) over growing seasons of five different years between 2008 and 2013 at this USDA site (19). We have also shown that the *PRI* is linearly related to canopy *LUE* over multiple growing seasons at this site (8,9,21,25). We previously quantified and reported the anisotropy of the *PRI* in our cornfield (7,8,20,22), as well as the anisotropy of the two individual *SIF* bands (SIF_{687}, SIF_{760}) (20). Here, we take our analysis a step further, to show that the *ANDI* for the *SIF* Ratio (SIF_{687}/SIF_{760}) displayed a mid-season peak that corresponded with the tower-derived *GEP* (Figure 5B) and was more strongly expressed in mid-mornings – when satellites typically view the Earth's surface, than in afternoons. Consequently, the nadir-acquired *SIF* Ratio and/or an index of *SPP* anisotropy for this *SIF* Ratio, appear to be more reliable predictors of the cornfield carbon dynamics across the season than either SIF_{760} or SIF_{687} alone.

Of particular note is the higher SIF_{760} associated with the canopy in early/moderate senescence (last three dates, Figure 3A). However, the corresponding tower-determined *GEP* was very low during senescence (Figure 5B). Clearly, *GEP* would be over-estimated if a linear assumption with SIF_{760} was applied for our cornfield. This demonstrates that the simple approach taken in some recent publications to estimate *GPP* based on a linear relationship to SIF_{760}, including cornfield crops (37), has limitations. We also show here that a fixed, unidirectional measurement of the spectral properties of the cornfield as they change diurnally and seasonally requires more than the far-red *SIF* to accurately estimate *GEP* at the local, crop scale (Figure 6). While we assume uniformity in the cornfield, it is possible that some of the variation in the relationship between *GEP* and the spectral data (Figure 6) was due to the fact that the flux tower and the FUSION tower viewed neighbouring sections of the cornfield. Still, our success in estimating *GEP* based entirely on spectral information required the inclusion of *PRI*, *NDVI*, and *APAR*, in addition to SIF_{760}. This spectral

suite allowed us to model the observed *GEP*, and accounted for 80% of seasonal and diurnal variability.

In this paper, we have clearly demonstrated that the observed canopy *SPP* anisotropy (represented by *ANDI*) of the *PRI* and *SIF* behave differently across the growing season, for morning *vs*. afternoons and for water treatments. The complementarity of these stress indices enables successful *GEP* estimates when combined, as shown here for *PRI* and SIF_{760} (plus two other spectral variables). We previously demonstrated a successful *GEP* retrieval with the combined use of the *PRI* and the red *SIF* (SIF_{687}) (9). Apparently, there are several potentially useful combinations of spectral information for estimating *GEP* and *LUE* from remote sensing approaches.

The capability to obtain these critical observations for both *SIF* quantities (SIF_{687}, SIF_{760}), their *SIF* Ratio (SIF_{687}/SIF_{760}), the full fluorescence spectrum (650-770 nm), the *PRI* and the *NDVI* will be provided by the recently-selected Earth Explorer Eight (EE-8) Phase A Mission, the Fluorescence Explorer (FLEX) satellite (38), to be developed and launched by the European Space Agency (ESA).

CONCLUSION

The findings of this research are summarized below:

a) Knowledge of the *BRDF* responses at different growth stages will enable researchers to better quantify the stress responses of the full canopy, as viewed with remote sensing tools.

b) The diurnal values for $SIF_{760} > SIF_{687}$ on all dates in this corn crop.

c) The *SPP ANDI* for anisotropy in these corn canopies was almost 50% higher for SIF_{760} than for SIF_{687}.

d) Although *ANDI* at both *SIF* wavelengths increased throughout the growth stages, it was not consistently related to either N or water treatments, or to time of day.

e) The FluoWat leaf-level measurements provided critical information on the partition of fluorescence into upward and downward emissions: upwelling spectra had approximately equal red and far-red peaks; whereas for transmitted downwelling spectra, the red peak at 685 nm << far-red peak at 740 nm.

f) The nadir-acquired *SIF* Ratio (SIF_{687}/SIF_{760}) and/or an index of *SPP* anisotropy for this *SIF* Ratio appear to be more reliable predictors of the cornfield carbon dynamics across the season than either SIF_{760} or SIF_{687} alone.

g) The observed canopy *SPP* anisotropy (represented by *ANDI*) of the *PRI* and *SIF* variables behave differently across the growing season, for morning *vs*. afternoons and for water treatments.

h) *GEP* was successfully estimated based entirely on spectral information, but SIF_{760} by itself was insufficient and required the inclusion of the *PRI*, the *NDVI*, and *APAR* in a 4-variable spectral suite, where modelled and observed *GEP* across the season were highly correlated ($r = 0.89$).

i) Apparently, there are several potentially useful combinations of *SIF* variables with additional spectral information for estimating *GEP* and *LUE* from remote sensing approaches.

ACKNOWLEDGEMENTS

This project received funding from three NASA Earth Science elements: Terrestrial Ecology, Remote Sensing, and Carbon Cycle (Program Manager, D. Wickland), and field operations support from USDA/BARC.

Students affiliated with the NASA/GSFC summer internship opportunities assisted: i), Undergraduates, Nicole Scott and Terrence Dickerson (Chemical Engineering), University of Maryland Baltimore County (UMBC) in Catonsville, MD USA; ii), David Lagomasino, Ph.D Environmental Studies, Florida International University, Miami, FL, USA; iii), Alexandra Anderson-Frey, Masters Candidate in Atmospheric Science, McGill University, Canada; iv), Kristine Frye, undergraduate in Engineering (Mary Washington College); v), this research was supported by an appointment to the NASA Postdoctoral Program at the Goddard Space Flight Center, administered by OakRidge Associated Universities through a contract with NASA.

REFERENCES

1 Deering D W, E M Middleton, J R Irons, B L Blad, E A Walter-Shea, C J Hays, C L Walthall, T F Eck, S P Ahmad & B P Banerjee, 1992. Prairie grassland bidirectional reflectances measured by different instruments at the FIFE site. Journal of Geophysical Research, Atmospheres, 97(D17): 18887-18903

2 Middleton E M, D W Deering & S P Ahmad, 1987. Surface anisotropy and hemispheric reflectance for a semiarid ecosystem, Remote Sensing of Environment, 23: 193-212

3 Schaaf C B, F Gao, A H Strahler, W Lucht, X Li, T Tsang, N C Strugnell, X Zhang, Y Jin, J-P Muller, P Lewis, M Barnsley, P Hobson, M Disney, G Roberts, M Dunderdale, C Doll, R. d'Entremont, B Hu, S Liang & J L Privette, 2002. First operational BRDF, albedo and nadir reflectance products from MODIS. Remote Sensing of Environment, 83: 135-148

4 Joiner J, Y Yoshida, A P Vasilkov, E M Middleton, P K E Campbell, Y Yoshida, A Kuze & L A Corp, 2012. Filling-in of near-infrared solar lines by terrestrial fluorescence and other geophysical effects: simulations and space-based observations from SCIAMACHY and GOSAT. Atmospheric Measurement Techniques, 5(4): 809-829

5 Campbell P K E, E M Middleton, L A Corp & M S Kim, 2008. Contribution of chlorophyll fluorescence to the apparent vegetation reflectance. Science of the Total Environment, 404: 433-439

6 Campbell P K E, E M Middleton, L A Corp, C van der Tol, K F Huemmrich, M P Cendrero-Mateo & J Leifelde, 2014. Diurnal dynamics and phenological changes in vegetation fluorescence, reflectance, and temperature indicative of vegetation photosynthetic properties and function. Proceedings, 5th Workshop on Remote Sensing of Vegetation Fluorescence, (ESA, CNES, Paris, France) 12 pp.

7 Cheng Y-B, E M Middleton, K F Huemmrich, Q Zhang, P K E Campbell, L A Corp, A L Russ & W P Kustas, 2010. Utilizing in situ directional hyperspectral measurements to validate bio-indicator simulations for a corn crop canopy. Ecological Informatics, 5: 330-338

8 Cheng Y-B, E M Middleton, K F Huemmrich, Q Zhang, L A Corp, P K E Campbell & W Kustas, 2011. Spectral bio-indicator simulations for tracking photosynthetic activities in a corn field. Proc. SPIE 8156, Remote Sensing and Modeling of Ecosystems for Sustainability VIII, 815607, 9 pp.

9 Cheng Y-B, E M Middleton, Q Zhang, K F Huemmrich, P K E Campbell, L A Corp, B D Cook, W P Kustas & C S Daughtry, 2013. Integrating solar induced fluorescence and the Photochemical Reflectance Index for estimating gross primary production in a cornfield. Remote Sensing, 5(12): 6857-6879

10 Corp L A, B D Cook, E M Middleton, Y-B Cheng, K F Huemmrich, P K E Campbell, 2010. FUSION: A Fully Ultraportable System for Imaging Objects in Nature. Proceedings, International Geoscience and Remote Sensing Symposium (IGARSS) (July 2010, Honolulu, HI) 5 pp.

11 Corp L A, M Hom, E M Middleton, K F Huemmrich, P K E Campbell & D R Landis, 2012, FUSION: Canopy tower system for remote sensing observations of terrestrial ecosystems, Instrument White Paper (last date accessed: 30 Nov 2015)

12 Corp L A, J E McMurtrey, E M Middleton, E W Chappelle & C S T Daughtry, 2003. Fluorescence sensing systems: *in vivo* detection of biophysical variations in field corn due to nitrogen supply. Remote Sensing of Environment, 86: 470-479

13 Corp L A, E M Middleton & P K E Campbell, 2007. Comparison of active and passive fluorescence techniques to evaluate plant growth and condition. Proceedings, 3rd International Workshop on Remote Sensing of Vegetation Fluorescence (Florence, Italy, February 2007) 4 pp.

14 Corp L A, E M Middleton & P K E Campbell, 2010. Remote sensing tools to evaluate plant growth and condition. Proceedings, 4nd International Workshop on Remote Sensing of Vegetation Fluorescence (Valencia, Spain, November 2010) 10 pp.

15 Corp L A, E M Middleton, P K E Campbell, K F Huemmrich, Y-B Cheng & C S T Daughtry, 2009. Remote sensing techniques to monitor nitrogen-driven carbon dynamics in field corn. Remote Sensing and Modeling of Ecosystems for Sustainability VI (OP502), SPIE International Symposium on Optical Engineering & Appl. (San Diego, CA, August 2009) 11 pp.

16 Corp L A, E M Middleton, P K E Campbell, K F Huemmrich, Y-B Cheng & C S T Daughtry, 2010. Spectral indices to monitor nitrogen driven carbon uptake in field corn. Journal of Applied Remote Sensing, 4: 0435555, 11 pp.

17 Krizek D T, E M Middleton, R K Sandhu & M S Kim, 2001. Evaluating UV-B effects and EDU protection in cucumber leaves using fluorescence images and fluorescence emission spectra. Journal of Plant Physiology, 158(1): 41-53

18 Middleton E M, E W Chappelle, T A Cannon, P Adamse & S J Britz, 1996. Initial assessment of physiological response to UV-B irradiation using fluorescence measurements. Journal of Plant Physiology, 148: 68-77

19 Middleton E M, Y-B Cheng, P K E Campbell, L A Corp, Q Zhang, K F Huemmrich, D R Landis, W P Kustas & A L Russ, 2014. Daily light use efficiency in a cornfield can be related to the canopy Red/Far-Red fluorescence ratio and leaf light use efficiency across a growing season. Proceedings, 5th Workshop on Remote Sensing of Vegetation Fluorescence, (ESA, CNES, Paris, France) 9 pp.

20 Middleton E M, Y-B Cheng, P K E Campbell, K F Huemmrich, Q Zhang, D R Landis, W P Kustas, C S T Daughtry & A L Russ, 2014. Directional hyperspectral observations to detect plant stress with the *PRI* and *SIF* in a cornfield. Proceedings, 4th Recent Advances in Quantitative Remote Sensing (RAQRS'IV) (Valencia, Spain, September 2014) 9 pp.

21 Middleton E M, Y-B Cheng, L A Corp, K F Huemmrich, P K E Campbell, Q Zhang, W P Kustas & A L Russ, 2009. Diurnal and seasonal dynamics of canopy-level solar-induced chlorophyll fluorescence and spectral reflectance indices in a cornfield. 6th EARSeL SIG Workshop on Imaging Spectroscopy (Tel-Aviv, Israel, March 2009) 12 pp.

22 Middleton E M, Y -B Cheng, L A Corp, K F Huemmrich, Q Zhang, P K E Campbell & W P Kustas, 2010. Diurnal and directional responses of chlorophyll fluorescence and *PRI* in a cornfield. Proceedings, 4th International Workshop on Remote Sensing of Vegetation Fluorescence (Valencia, Spain, November 2010) 5 pp.

23 Middleton E M, L A Corp & P K E Campbell, 2007. Synthesis of leaf-level fluorescence, reflectance, and photosynthesis with linkage to canopy solar induced fluorescence, Proceedings,

3rd International Workshop on Remote Sensing of Vegetation Fluorescence (Florence, Italy, Feb. 2007) 4 pp.

24 Middleton E M, L A Corp & P K E Campbell, 2008. Comparison of measurements and FluorMOD simulations for solar induced chlorophyll fluorescence and reflectance of a corn crop under nitrogen treatments. International Journal of Remote Sensing, Special Issue., Second International Symposium on Recent Advances in Quantitative Remote Sensing (RAQRSII), 29(17): 5,193-5,213

25 Middleton E M, L A Corp, P K E Campbell & C S T Daughtry, 2006. Relating canopy hyperspectral reflectance and fluorescence indices to carbon related parameters. Proceedings, Second Symposium on Recent Advances in Quantitative Remote Sensing II (RAQRSII) (Valencia, Spain, Sept. 2006) 6 pp.

26 Middleton E M, M S Kim, D T Krizek & R B K Bajwa, 2005. Evaluating UV B effects and EDU protection in soybean leaves using fluorescence. Symposium in Print on the Effects of Ultraviolet Radiation on Terrestrial Ecosystems. Photochemistry and Photobiology, 81: 1075-1085

27 Middleton E M, J E McMurtrey, P K E Campbell, L A Corp, L M Butcher & E W Chappelle, 2003. Optical and fluorescence properties of corn leaves from different nitrogen regimes. SPIE Vol 4879, Remote Sensing for Agriculture, Ecosystems, and Hydrology IV, M. Owe, G. D'Urso, L. Toulios, Eds., pp. 72-83

28 Middleton E M, J E McMurtrey, L A Corp, P K E Campbell, L M Butcher & E W Chapelle, 2004. Nitrogen stress in corn as detected and monitored by fluorescence and optical reflectance measurements, Remote Sensing for Agriculture and the Environment, Organization for Economic and Cooperative Development (OECD), S Stamatiadis, J M Lynch, and J S Schepers (Eds.), published by Peripheral Editions for the Office of Economic and Cooperative Development (OECD) and the Gaia Center of the Goulandris Natural History Museum, Athens, Greece, pp. 150-173

29 van der Tol C, J A Berry, P K E Campbell & U Rascher, 2015. Models of fluorescence and photosynthesis for interpreting measurements of solar-induced chlorophyll fluorescence. Journal of Geophysical Research: Biogeosciences, 119(12): 2312-2327

30 Verhoef V, C van der Tol & E M Middleton, 2014. Vegetation canopy fluorescence and reflectance retrieval by model inversion using optimization. Proceedings, 5th Workshop on Remote Sensing of Vegetation Fluorescence (ESA, CNES, Paris, France) 12 pp.

31 Middleton E M, Y-B Cheng, T Hilker, T A Black, P Krishnan, N C Coops & K F Huemmrich, 2009. Linking foliage spectral responses to canopy level ecosystem photosynthetic light use efficiency at a Douglas-fir forest in Canada. Canadian Journal of Remote Sensing, 35: 166-188

32 Meroni M, L Busetto, R Colombo, L Guanter, J Moreno & W Verhoef, 2010. Performance of spectral fitting methods for vegetation fluorescence quantification, Remote Sensing of Environment, 114(2): 363-374

33 Cook B D, K J Davis, W Wang, A R Desai, B W Berger, R M Teclaw, J M Martin, P Bolstad, P Bakwin, C Yi & W Heilman, 2004. Carbon exchange and venting anomalies in an upland deciduous forest in northern Wisconsin, USA. Agricultural and Forest Meteorology, 126(3-4): 271-295

34 Van Wittenberghe S, S L Alonso, J Verrelst, I Hermans, J Delegido, F Veroustraete, R Valcke, J Moreno & R Samson, 2013. Upward and downward solar-induced chlorophyll fluorescence yield indices of four tree species as indicators of traffic pollution in Valencia. Environmental Pollution, 173: 29-37

35 Middleton E M, K F Huemmrich, Y-B Cheng & H A Margolis, 2011. Spectral bio-indicators of photosynthetic efficiency and vegetation stress. In: P S Thekabail, J G Lyon and A Huete (Editors), Hyperspectral Remote Sensing of Vegetation (CRC Press) pp. 265-288

36 Porcar-Castell A, E Tyystjärv, J Atherton, C van der Tol, J Flexas, E E Pfündel, J Moreno, C Frankenberg & J A Berry, 2014. Linking chlorophyll-a fluorescence to photosynthesis for remote sensing applications: mechanisms and challenges, Journal of Experimental Botany, 65(15): 4065-4095

37 Guanter L, Y Zhang, M Jung, J Joiner, M Voigt, J A Berry, C Frankenberg, A R Huete, P Zarco-Tejada, J E Lee, M Susan Moran, G Ponce-Campos, C Beer, G Camps-Valls, N Buchmann, D Gianelle, Katja Klumpp, Alessandro Cescatti, John M. Baker & T J Griffis, 2014. Global and time-resolved monitoring of crop photosynthesis with chlorophyll fluorescence. PNAS, 111(14): E1327-E1333

38 European Space Agency (ESA), 2008. Candidate Earth Explorer Core Mission. FLEX – Fluorescence Explorer. Report for Assessment, ESA SP-1313/4 (ESTEC, Noordwijk, The Netherlands) 126 pp.